Contact Dynamics of a Spherical Joint and a Jointed Truss-Cell System

H. S. Tzou* and Y. Rong†
University of Kentucky, Lexington, Kentucky 40506

This paper presents a mathematical modeling and stochastic simulation study of a three-dimensional spherical joint, a design feature of importance to a class of deployable space structures. An analytical model of the joint including friction and clearance effects is studied, and a system equation with time-variant coefficient matrices is then derived. A parametric study, including joint clearance size, joint rigidity/damping, and link elasticity/damping, of a jointed truss-cell model is investigated. The friction is assumed to be a normally distributed random variable and the external excitation is also treated random in a stochastic simulation study using an auto-regressive moving average (ARMA) model. This study shows that the joint dynamic contacts are affected by joint surface condition (stiffness/damping), joint clearance, link stiffness/damping, excitation, etc. Friction contacts dominate the system dynamics when the clearance is small and normal contacts dominate when the clearance is large.

Nomenclature

A	= amplitude of joint friction force
$[A]$	= coefficient matrix
A_{fl}, A_{xt}	= random disturbance data series
B	= delay operator
C_p, C_{p1}, C_{p2}	= contact damping coefficients
C_s, $[C_s]$	= equivalent link damping coefficient and matrix
D	= constant coefficient
dt	= time increment
F_c, F_{cx}, F_{cy}, F_{cz}	= joint contact force vector and its components
F_f, F_{fx}, F_{fy}, F_{fz}	= joint friction force vector and its components
$H(B)$	= system transfer function
$[I]$	= unit matrix
I_x, I_y, I_z	= mass moments of inertia in X, Y and Z directions, respectively
i, j, k	= unit vectors in X, Y, and Z directions, respectively
K_p, K_{p1}, K_{p2}	= contact stiffness
K_s, $[K_s]$	= equivalent link stiffness and matrix
$[M_s]$	= equivalent link mass matrix
m, $[M]$	= joint mass and matrix
R_1, R_2	= radii of the central ball and socket of a spherical joint
$[Rm]$	= equivalent damping matrix
$R(u)$	= normally distributed random variable and u is a uniformly distributed random variable
$S(\lambda)$	= step function
$\{U\}$, $\{V\}$	= equivalent forcing vector
U_p	= relative vibration displacement
u_1, u_2, u_3, u_4, u_5, u_6	= coefficients in system equation
$\{W_1\}$, $\{W_2\}$, $\{W_3\}$	= vibration displacement vector
X_1, X_2, X_3	= vibration displacements in x direction
X_t	= system output time series data
Y_1, Y_2, Y_3	= vibration displacements in y direction
Z_1, Z_2, Z_3	= vibration displacements in z direction
$\{Z\}$, z_1, z_2, z_3,..., z_{12}	= intervariable vector and its components
β_{nk}	= damping ratio in kth mode
Δ^*	= time interval
δ, δ_1, δ_2	= joint clearances
$[\eta]$	= time-variant coefficient matrix in system equation
$\{\eta\}$	= time-variant coefficient vector in system equation
$\theta_i(B)$	= moving average (MA) parameters, $i = 1,2$
θ_x, θ_y, θ_z	= contact angle and its directional components
λ	= relative penetration displacement
λ_k, λ_k^*	= characteristic root of system transer function
μ, μ_c	= friction coefficient
σ_x, σ_y, σ_z	= coefficients in friction force expression
φ_{ix}, φ_{iy}, φ_{iz}	= rotation angle, $i = 1, 2$
$\varphi_{ij}(B)$	= auto-regressive (AR) parameters, $i = 1,2$
ω_{nk}	= kth mode natural frequency
$[\omega^2]$	= equivalent stiffness matrix
Subscripts	
P	= contact point
x,y,z	= coordinate coefficients

Received Aug. 21, 1989; revision received Feb. 9, 1990; presented as Paper 90-0939 at the AIAA 31st Structures, Structural Dynamics and Materials Conference, Long Beach, CA, April 2-4, 1990.

*Assistant Professor, Department of Mechanical Engineering; Research Faculty, Center for Robotics and Manufacturing Systems. Member AIAA.

†Postdoctoral Research Associate, Department of Mechanical Engineering; currently, Assistant Professor, Southern Illinois University.

Introduction

JOINTED structural and mechanical systems, such as trusses, mechanisms, machines, etc., have been around and studied for a long time. Recently, due to the rapid development of large flexible deployable space structures, joint dynamic characteristics have become even more important to their high-precision and high-performance operations.[1] The mechanical clearance inside a joint can induce dynamic contacts when the jointed structure is subjected to a sudden maneuver or external excitations; the internal contact can hamper

its operation accuracy, introduce noise and vibration, accelerate wear and fatigue, which results in system instability and premature failures, etc.[2] This paper presents a three-dimensional theoretical model of a spherical joint (including the dynamic effects of clearance and friction) and a stochastic simulation of a jointed structure—a jointed truss-cell model.

Dynamics of jointed space structures have been studied increasingly in recent years. Foelsche et al.[3] recently proposed a new linearization technique to study the transient response of joint-dominated space structures. Crawley and O'Donnell[4] investigated nonlinear joint properties using a force-state mapping technique.[4] Tzou[5] studied the multibody nonlinear dynamics and controls of joint-dominated flexible structures. Rong et al.[6] developed a two-dimensional pin joint model including contact and friction effects. Composite joints, "sloppy" joints, and bolted joints were also studied and evaluated by a number of researchers.[7-9] In this paper, emphases are placed on 1) development of a three-dimensional spherical joint model including dynamic contacts and frictions and 2) dynamic analysis of a jointed truss-cell model, a fundamental unit in a complicated space truss system, subjected to random excitation using a stochastic simulation technique.

Joint-dominated space structures could be exposed to excitations that are random in nature. Besides, wear and aging could also change joint characteristics and result in irregular surfaces with localized joint parameters. In this study, a three-dimensional joint model is first developed based on a contact force analysis. The derived analytical model has time-variant coefficient matrices depending on relative displacements, contact angles, step functions, etc. Then, a recursive algorithm is implemented to solve the system equations and to calculate joint contact dynamics. A stochastic simulation approach using an autoregressive moving average (ARMA) process[6,10] is also proposed to study the dynamic characteristics and responses of a flexible jointed structure—a truss-cell structure. The technique is based on the system differential equations and a stochastic process theory. A stochastic simulation program is developed to estimate the system performances when system parameters (e.g., excitation amplitude/frequency, clearance size, joint stiffness/damping, and link stiffness/damping) are specified. Dynamic contact responses of the truss-cell model with various joint parameters are presented and studied.

Theory

A joint-dominated deployable structural system usually consists of a number of elastic links connected by joints in which a small joint clearance is reserved to allow relative motion of connected links. In this section, a mathematical model of a three-dimensional spherical joint is developed, and then this model is extended to a link/socket and ball/link physical system, which will be studied using a stochastic simulation technique in a later section.

System Definition

A spherical joint, a ball (denoted as 2) inside a socket (denoted as 1) at the end of two links, is illustrated in Fig. 1. The point O is the center and P is an arbitrary contact point. A joint clearance δ is defined as the difference of the inner radius of the socket and the outer radius of the ball, i.e., $\delta = R_1 - R_2$.

When the jointed system is moving and/or excited by external excitations, the ball comes in contact with the socket when the relative displacement exceeds the joint clearance. A set of equivalent contact stiffness/damping, C_p and K_p, is assumed to represent the joint contact action. This joint contact can affect the dynamic characteristics of the entire jointed system. It is assumed that the joint contact has two major components: 1) normal and 2) tangential. The first one contributes a normal contact and the second a friction contact. It is also assumed that the clearance is large enough to allow relative motion so that the joint "sticktion" is not considered. Figure 2 illustrates a joint coordinate system that also defines contact location (P), contact forces, angular rotations, etc. In the later derivation, the normal and friction contacts are discussed separately and followed by a formulation of system equations.

Normal Contact

Define $(X_1, Y_1, Z_1, \varphi_{1x}, \varphi_{1y}, \varphi_{1z})$ and $(X_2, Y_2, Z_2, \varphi_{2x}, \varphi_{2y}, \varphi_{2z})$ as the translational and rotational motions of the link/socket and the ball, respectively. The normal contact force $\bar{F}_c$ contribnted by joint stiffness and damping at point "P" can be expressed as

$$\begin{aligned}\bar{F}_c &= F_{cx}i + F_{cy}j + F_{cz}k \\ &= -i[C_p\dot{U}_p + K_p(U_p-\delta)\cos\theta_x S(\lambda) \\ &\quad -j[C_p\dot{U}_p + K_p(U_p-\delta)]\cos\theta_y S(\lambda) \\ &\quad -k[C_p\dot{U}_p + K_p(U_p-\delta)]\cos\theta_z S(\lambda)\end{aligned} \tag{1}$$

where U_p and $\dot{U}_p$ are the relative displacement and velocity in the contact direction, respectively, and they are defined as

$$\begin{aligned}\bar{U}_p &= \Delta Xi + \Delta Yj + \Delta Zk \\ &= (X_2-X_1)i + (Y_2-Y_1)j + (Z_2-Z_1)k;\end{aligned} \tag{2a}$$

$$\begin{aligned}U_p &= |\bar{U}_p| \\ &= [(X_2-X_1)^2 + (Y_2-Y_1)^2 + (Z_2-Z_1)^2]^{1/2} \\ &= (X_2-X_1)\cos\theta_x + (Y_2-Y_1)\cos\theta_y + (Z_2-Z_1)\cos\theta_z\end{aligned} \tag{2b}$$

$$\dot{U}_p = (\dot{X}_2-\dot{X}_1)\cos\theta_x + (\dot{Y}_2-\dot{Y}_1)\cos\theta_y + (\dot{Z}_2-\dot{Z}_1)\cos\theta_z \tag{2c}$$

The contact direction is defined by its directional cosine functions:

$$\cos\theta_x = \frac{X_2-X_1}{[(X_2-X_1)^2+(Y_2-Y_1)^2+(Z_2-Z_1)^2]^{1/2}} \tag{3a}$$

$$\cos\theta_y = \frac{Y_2-Y_1}{[(X_2-X_1)^2+(Y_2-Y_1)^2+(Z_2-Z_1)^2]^{1/2}} \tag{3b}$$

$$\cos\theta_z = \frac{Z_2-Z_1}{[(X_2-X_1)^2+(Y_2-Y_1)^2+(Z_2-Z_1)^2]^{1/2}} \tag{3a}$$

$S(\lambda)$ is a step function and is defined as

$$S(\lambda) = \begin{cases} 0, & \text{if } \lambda < 0 \\ 1, & \text{if } \lambda \geq 0 \end{cases} \tag{4}$$

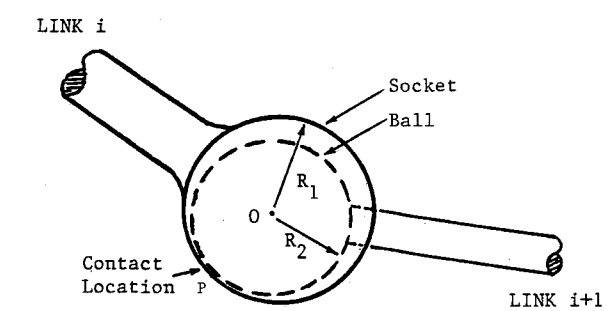

Fig. 1 Cross section of a three-dimensional spherical ball/socket joint.

$$\lambda = U_p - \delta = [(X_2 - X_1)^2 + (Y_2 - Y_1)^2 + (Z_2 - Z_1)^2]^{1/2} - \delta \quad (5)$$

Friction Contact

The friction force $\bar{F}_f$ can be decomposed into F_{fx}, F_{fy}, F_{fz} and in the direction of x, y, and z:

$$\bar{F}_f = F_{fx}i + F_{fy}j + F_{fz}k \quad (6)$$

The direction of the friction force is opposite to the tangential velocity (at contact point P) and perpendicular to the relative displacement and angular velocity vectors at the contact point. Thus,

$$\bar{F}_f \perp \bar{U}_p, \qquad \bar{F}_f \perp \Delta\dot{\bar{\varphi}}$$

where U_p is the relative displacement vector defined in Eq. (2a), and $\Delta\dot{\bar{\varphi}}$ is the relative angular velocity vector of the ball in the joint,

$$\Delta\dot{\bar{\varphi}} = \Delta\dot{\varphi}_x i + \Delta\dot{\varphi}_y j + \Delta\dot{\varphi}_z k$$
$$= (\dot{\varphi}_{2x} - \dot{\varphi}_{1x})i + (\dot{\varphi}_{2y} - \dot{\varphi}_{1y})j + (\dot{\varphi}_{2z} - \dot{\varphi}_{1z})k \quad (7)$$

Thus, the friction force is defined as

$$\bar{F}_f = A(\bar{U}_p \times \Delta\dot{\bar{\varphi}})$$
$$= A[(\Delta Y\Delta\dot{\varphi}_z - \Delta Z\Delta\dot{\varphi}_y)i + (\Delta Z\Delta\dot{\varphi}_x - \Delta X\Delta\dot{\varphi}_z)j$$
$$+ (\Delta X\Delta\dot{\varphi}_y - \Delta Y\Delta\dot{\varphi}_x)k] \quad (8)$$

where A is related to the amplitude of friction force. Consider the following relationship,

$$F_{fx}^2 + F_{fy}^2 + F_{fz}^2 = \mu^2 F_c^2 \quad (9)$$

where μ is the friction coefficient. The amplitude can be determined by

$$A = \frac{\mu|F_c|}{[(\Delta Y\Delta\dot{\varphi}_z - \Delta Z\Delta\dot{\varphi}_y)^2 + (\Delta Z\Delta\dot{\varphi}_x - \Delta X\Delta\dot{\varphi}_z)^2 + (\Delta X\Delta\dot{\varphi}_y - \Delta Y\Delta\dot{\varphi}_x)^2]^{1/2}} \quad (10)$$

The friction forces in three directions can be expressed as

$$F_{fx} = \mu\sigma_x|F_c|$$
$$= \mu\sigma_x[C_p\dot{U}_p + K_p(U_p - \delta)]S(\lambda) \quad (11a)$$

$$F_{fy} = \mu\sigma_y|F_c|$$
$$= \mu\sigma_y[C_p\dot{U}_p + K_p(U_p - \delta)]S(\lambda) \quad (11b)$$

$$F_{fz} = \mu\sigma_z|F_c|$$
$$= \mu\sigma_z[C_p\dot{U}_p + K_p(U_p - \delta)]S(\lambda) \quad (11c)$$

where

$$\sigma_x = \frac{\Delta Y\Delta\dot{\varphi}_z - \Delta Z\Delta\dot{\varphi}_y}{[(\Delta Y\Delta\dot{\varphi}_z - \Delta Z\Delta\dot{\varphi}_y)^2 + (\Delta Z\Delta\dot{\varphi}_x - \Delta X\Delta\dot{\varphi}_z)^2 + (\Delta X\Delta\dot{\varphi}_y - \Delta Y\Delta\dot{\varphi}_x)^2]^{1/2}} \quad (12a)$$

$$\sigma_y = \frac{\Delta Z\Delta\dot{\varphi}_x - \Delta X\Delta\dot{\varphi}_z}{[(\Delta Y\Delta\dot{\varphi}_z - \Delta Z\Delta\dot{\varphi}_y)^2 + (\Delta Z\Delta\dot{\varphi}_x - \Delta X\Delta\dot{\varphi}_z)^2 + (\Delta X\Delta\dot{\varphi}_y - \Delta Y\Delta\dot{\varphi}_x)^2]^{1/2}} \quad (12b)$$

$$\sigma_z = \frac{\Delta X\Delta\dot{\varphi}_y - \Delta Y\Delta\dot{\varphi}_x}{[(\Delta Y\Delta\dot{\varphi}_z - \Delta Z\Delta\dot{\varphi}_y)^2 + (\Delta Z\Delta\dot{\varphi}_x - \Delta X\Delta\dot{\varphi}_z)^2 + (\Delta X\Delta\dot{\varphi}_y - \Delta Y\Delta\dot{\varphi}_x)^2]^{1/2}} \quad (12c)$$

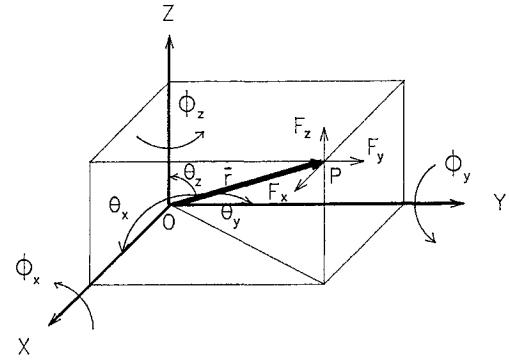

Fig. 2 Joint coordinate system.

Up to this point, the normal contact and the friction contact are discussed and their force components are formulated. Next, the system equation of the ball/socket/link system will be derived. Note that rotational friction and joint slicking were not considered in the derivation.

System Equation

The system equation of the contact pair, the ball and the socket/link, can be expressed as

$$m\ddot{X}_2 = F_{cx} + F_{fx} \quad (13a)$$

$$m\ddot{Y}_2 = F_{cy} + F_{fy} \quad (13b)$$

$$m\ddot{Z}_2 = F_{cz} + F_{fz} \quad (13c)$$

$$I_z\ddot{\varphi}_{2z} - (I_x - I_y)\dot{\varphi}_{2x}\dot{\varphi}_{2y} = -F_{fx}R_2\cos\theta_y + F_{fy}R_2\cos\theta_x \quad (13d)$$

$$I_y\ddot{\varphi}_{2y} - (I_z - I_x)\dot{\varphi}_{2x}\dot{\varphi}_{2z} = F_{fx}R_2\cos\theta_z - F_{fz}R_2\cos\theta_x \quad (13e)$$

$$I_x\ddot{\varphi}_{2x}-(I_y-I_z)\dot{\varphi}_{2y}\dot{\varphi}_{2z}=F_{fz}R_2\cos\theta_y-F_{fy}R_2\cos\theta_z \tag{13f}$$

where m is the ball mass in the joint and I_x, I_y, and I_z are the mass moments of inertia in x, y, and z directions, respectively. In the case of a spherical ball, i.e., $I_x=I_y=I_z$, so that the gyroscopic effect can be neglected and the earlier system equation can be written in a matrix form:

$$\begin{bmatrix} m & 0 & 0 & 0 & 0 & 0 \\ 0 & m & 0 & 0 & 0 & 0 \\ 0 & 0 & m & 0 & 0 & 0 \\ 0 & 0 & 0 & I_z & 0 & 0 \\ 0 & 0 & 0 & 0 & I_y & 0 \\ 0 & 0 & 0 & 0 & 0 & I_x \end{bmatrix} \begin{bmatrix} \ddot{X}_2 \\ \ddot{Y}_2 \\ \ddot{Z}_2 \\ \ddot{\varphi}_{2z} \\ \ddot{\varphi}_{2y} \\ \ddot{\varphi}_{2x} \end{bmatrix}$$

$$+C_pS(\lambda)\begin{bmatrix} \cos\theta_x u_1 & \cos\theta_y u_1 & \cos\theta_z u_1 & 0 & 0 & 0 \\ \cos\theta_x u_2 & \cos\theta_y u_2 & \cos\theta_z u_2 & 0 & 0 & 0 \\ \cos\theta_x u_3 & \cos\theta_y u_3 & \cos\theta_z u_3 & 0 & 0 & 0 \\ \cos\theta_x u_4 & \cos\theta_y u_4 & \cos\theta_z u_4 & 0 & 0 & 0 \\ \cos\theta_x u_5 & \cos\theta_y u_5 & \cos\theta_z u_5 & 0 & 0 & 0 \\ \cos\theta_x u_6 & \cos\theta_y u_6 & \cos\theta_z u_6 & 0 & 0 & 0 \end{bmatrix} \begin{bmatrix} \Delta\dot{X} \\ \Delta\dot{Y} \\ \Delta\dot{Z} \\ \Delta\dot{\varphi}_z \\ \Delta\dot{\varphi}_y \\ \Delta\dot{\varphi}_x \end{bmatrix}$$

$$+K_pS(\lambda)\begin{bmatrix} \cos\theta_x u_1 & \cos\theta_y u_1 & \cos\theta_z u_1 & 0 & 0 & 0 \\ \cos\theta_x u_2 & \cos\theta_y u_2 & \cos\theta_z u_2 & 0 & 0 & 0 \\ \cos\theta_x u_3 & \cos\theta_y u_3 & \cos\theta_z u_3 & 0 & 0 & 0 \\ \cos\theta_x u_4 & \cos\theta_y u_4 & \cos\theta_z u_4 & 0 & 0 & 0 \\ \cos\theta_x u_5 & \cos\theta_y u_5 & \cos\theta_z u_5 & 0 & 0 & 0 \\ \cos\theta_x u_6 & \cos\theta_y u_6 & \cos\theta_z u_6 & 0 & 0 & 0 \end{bmatrix} \begin{bmatrix} \Delta X \\ \Delta Y \\ \Delta Z \\ \Delta\varphi_z \\ \Delta\varphi_y \\ \Delta\varphi_x \end{bmatrix}$$

$$=K_p\delta S(\lambda)\begin{bmatrix} u_1 \\ u_2 \\ u_3 \\ u_4 \\ u_5 \\ u_6 \end{bmatrix} \tag{14}$$

where u is defined as

$$u_1=\cos\theta_x-\mu\sigma_x \tag{15a}$$

$$u_2=\cos\theta_y-\mu\sigma_y \tag{15b}$$

$$u_3=\cos\theta_z-\mu\sigma_z \tag{15c}$$

$$u_4=\mu R_2(\sigma_x\cos\theta_y-\sigma_y\cos\theta_x) \tag{15d}$$

$$u_5=\mu R_2(\sigma_z\cos\theta_x-\sigma_x\cos\theta_z) \tag{15e}$$

$$u_6=\mu R_2(\sigma_y\cos\theta_z-\sigma_z\cos\theta_y) \tag{15f}$$

Or, the equation can be simply expressed as:

$$[M]\{\ddot{W}_2\}+C_pS(\lambda)[\eta]\{\dot{W}_2-\dot{W}_1\}+K_pS(\lambda)[\eta]\{W_2-W_1\}$$
$$=K_p\delta S(\lambda)\{\eta'\} \tag{16}$$

where $[M]$ denotes the overall mass matrix, $\{W_2\}=\{X_2\ Y_2\ Z_2\ \varphi_{2z}\ \varphi_{2y}\ \varphi_{2x}\}^T$, and $\{W_1\}=\{X_1\ Y_1\ Z_1\ \varphi_{1z}\ \varphi_{1x}\ \varphi_{1y}\ \varphi_{1z}\}^T$; the superscript T denotes the matrix transponse.

$$[\eta]=\begin{bmatrix} \cos\theta_x u_1 & \cos\theta_y u_1 & \cos\theta_z u_1 & 0 & 0 & 0 \\ \cos\theta_x u_2 & \cos\theta_y u_2 & \cos\theta_z u_2 & 0 & 0 & 0 \\ \cos\theta_x u_3 & \cos\theta_y u_3 & \cos\theta_z u_3 & 0 & 0 & 0 \\ \cos\theta_x u_4 & \cos\theta_y u_4 & \cos\theta_z u_4 & 0 & 0 & 0 \\ \cos\theta_x u_5 & \cos\theta_y u_5 & \cos\theta_z u_5 & 0 & 0 & 0 \\ \cos\theta_x u_6 & \cos\theta_y u_6 & \cos\theta_z u_6 & 0 & 0 & 0 \end{bmatrix} \tag{17a}$$

$$\{\eta'\}=\{u_1\ u_2\ u_3\ u_4\ u_5\ u_6\}^T \tag{17b}$$

It should be noted that the $[\eta]$ and $\{\eta'\}$ are functions of the contact point P, which is determined by any two of the angles θ_x, θ_y, and θ_z.

If a two-link system, link/socket-ball-link configuration, is considered (Fig. 1), Eq. (16) can be written as

$$[M]\{\ddot{W}_2\}+C_{p1}S(\lambda)[\eta_1]\{\dot{W}_2-\dot{W}_1\}+C_{p2}S(\lambda_2)[\eta_2]\{\dot{W}_2-\dot{W}_3\}$$
$$+K_{p1}S(\lambda_1)[\eta_1]\{W_2-W_1\}+K_{p2}S(\lambda_2)[\eta_2]\{W_2-W_3\}$$
$$=K_{p1}\delta_1S(\lambda_1)\{\eta_1'\}+K_{p2}S(\lambda_2)\delta_2\{\eta_2'\} \tag{18}$$

where $\{W_3\}$ is the displacement vector of the second link, and δ_2 is the clearance between the ball and the second link. For a physical system, the δ_2 should be zero (i.e., the ball is fixed to the second link). Thus, $\{W_2\}=\{W_3\}$, and Eq. (18) becomes

$$[M_s]\{\ddot{W}_2\}+C_pS(\lambda)[\eta]\{\dot{W}_2-\dot{W}_1\}+[C_S]\{\dot{W}_2\}$$
$$+K_pS(\lambda)[\eta]\{W_2-W_1\}+[K_S]\{W_2\}=K_p\delta S(\lambda)\{\eta'\} \tag{19}$$

where $[M_s]$, $[C_s]$ and $[K_s]$ are, respectively, the equivalent mass, linear damping, and stiffness matrices of the joint, which can be regarded as part of the second link. This is a nonlinear model because of not only the step functions but also the time-variant coefficient matrix $[\eta]$. If some of the variables, Z_i, φ_{ix}, and φ_{iy}, in Eq. (19), are set to zero, the system equation can be simplified to a two-dimensional joint model.[6]

Stochastic Simulation Technique

In order to solve the system equation, the system is first linearized by treating it as a quasistatic problem so that a recursive algorithm can be developed. Then, the system equation is randomized to include surface irregularity and random excitation effects; the system characteristics are evaluated using a stochastic simulation technique—an ARMA process.[6,10]

Linearization of System Equation

In the previous elastic joint model, if the motion of the first link (X_1, Y_1, Z_1, φ_{1x}, φ_{1y}, φ_{1z}) is taken as an input variable, the output, second link,s motion (X_2, Y_2, Z_2, φ_{2x}, φ_{2y}, φ_{2z}) can be evaluated by a recursive algorithm. Rewriting the system equation yields

$$\{\ddot{W}_2\}+[R_m]\{\dot{W}_2\}+[\omega^2]\{W_2\}=\{U\} \tag{20}$$

where

$$[R_m]=C_pS(\lambda)[M_s]^{-1}[\eta]+[M_s]^{-1}[C_s]; \tag{21a}$$

$$[\omega^2]=K_pS(\lambda)[M_s]^{-1}[\eta]+[M_s]^{-1}[K_s]; \tag{21b}$$

$$\{U\}=\{U(W_1)\}$$
$$=K_p\delta S(\lambda)[M_s]^{-1}\{\eta'\}+C_pS(\lambda)[M_s]^{-1}[\eta]\{W_1\}$$
$$+K_pS(\lambda)[M_s]^{-1}[\eta]\{W_1\} \tag{21c}$$

Define a state-variable vector $\{Z\}$ as

$$\{z_1, z_2, z_3, z_4, z_5, z_6, z_7, z_8, z_9, z_{10}, z_{11}, z_{12}\}^T = \{X_2, Y_2, Z_2, \varphi_{2x}, \varphi_{2y}, \varphi_{2z}, \dot{X}_2, \dot{Y}_2, \dot{Z}_2, \dot{\varphi}_{2x}, \dot{\varphi}_{2y}, \dot{\varphi}_{2z}\}^T \quad (22)$$

Then, the system equation becomes a first-order state equation:

$$\{\dot{Z}\} = \begin{bmatrix} [0] & [I] \\ -[\omega^2] & -[R_m] \end{bmatrix} \{Z\} + \begin{bmatrix} \{0\} \\ \{U\} \end{bmatrix} \quad (23a)$$

or

$$\{\dot{Z}\} = [A]\{Z\} + \{V\} \quad (23b)$$

If the current vibration state is known at any given time instant (i.e., given $\{Z(n)\}$ at step n), the matrix $[\eta]$ is considered as a constant so that the matrix $[A]$ becomes a constant matrix. Thus, the value of $\{Z(n+1)\}$ at step $(n+1)$ can be estimated by the following recursive function

$$\{Z(n+1)\} = ([A(n)]\{Z(n)\} + \{V(n)\})^* dt + \{Z(n)\} \quad (24)$$

where dt is a time interval.

Randomization of Joint Variables

As discussed earlier, the joint surface properties could become irregular due to wear and aging, and the mechanical friction could also be random.[11] Thus, the joint friction force can be rewritten as

$$F_f = \mu F_c \quad (25)$$

where F_c is the normal contact force; μ is a random friction coefficient and it is defined as

$$\mu = \mu_c + DR(u) \quad (26)$$

where μ_c is a nominal friction coefficient related to the material/surface property; $R(u)$ is a normally distributed random variable with zero mean value, which is estimated from a uniform random variable generator;[12] and D is a constant that controls the variation of friction force. In order to simulate the complex working environment/condition of a jointed system, e.g., a jointed space structure, a random excitation is also considered in the simulation process.

Stochastic Simulation Structure

In order to evaluate the dynamic characteristics of jointed systems, a stochastic simulator is designed based on the developed dynamic contact model of elastic joints and the stochastic process theory. The simulator primarily consists of two parts: 1) time-history analysis and 2) system parameter analysis.

First, the system parameters need to be specified, and then the time-history data are generated based on the model discussed earlier. From these data, the joint dynamic contact pattern can be observed in the time domain. The time-history data can also be fitted into an ARMA model so that the system dynamic characteristics, such as natural frequencies and damping ratios, can be determined. An ARMA model is expressed as[13,14]

$$\varphi_{11}(B)\, X_t = \varphi_{12}(B)\, F_t + \theta_1(B)\, A_{xt} \quad (27a)$$

$$\varphi_{22}(B)\, F_t = \theta_2(B)\, A_{ft} \quad (27b)$$

where F_t is a data series representing the vibration displacement of link 1, as an input; X_t is a data series representing the vibration displacement of link 2 as an output; A_{ft} and A_{xt} are disturbances to input and output, and considered as white noises; φ_{ij} and θ_i are polynomial functions of B, which are related to the ARMA parameters, respectively; and B is a time delay operator, i.e., $BX_t = X_{t-1}$. The transfer function is defined by

$$H(B) = \frac{\varphi_{12}(B)}{\varphi_{11}(B)} \quad (28)$$

Then, the natural frequencies ω_{nk} and damping ratios β_{nk} of the jointed system can be estimated using the impulse invariance principle:

$$\omega_{nk} = \frac{1}{\Delta^*}[\ell n(\lambda_k)\ell n(\lambda_k^*)]^{1/2} \quad (29a)$$

$$\beta_{nk} = \frac{-\ell n(\lambda_k \lambda_k^*)}{2[\ell n(\lambda_k)\ell n(\lambda_k^*)]^{1/2}} \quad (29b)$$

Simulation Study of a Jointed Truss-Cell Model

A jointed truss-cell unit can be considered as the basic component of many large jointed flexible space structural systems, e.g., deployable space structure.[6] The cross section of a basic three-dimensional truss-cell model is illustrated in Fig. 3a, in which two links (designated as 1 and 3) are connected by a joint (designated as 2). As discussed earlier, the ball is one end of one link and the socket is integrated with the other link. Thus, the truss-cell model can be further simplified as an equivalent spring-joint mass-link (mass, spring, and damper) system, as shown in Fig. 3b.

Note that the joint clearance, the contact stiffness/damping, the equivalent link mass, and external excitations are illustrated in the figures. Also note that only planar excitations are considered in the simulation study. A constant contact damping ratio (which is related to the material property) and sine—shaped contact stiffness (considering the stiffness variation in different contact direction θ of joint) are also assumed in the simulation model. The values of system parameters are determined based on the analysis and experi-

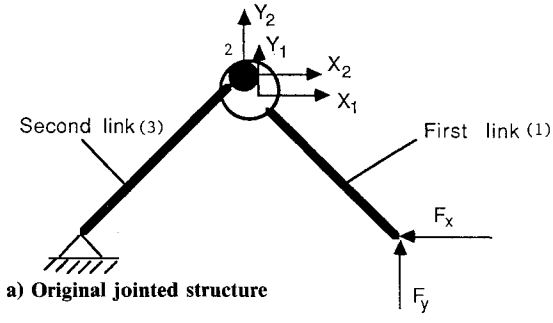

a) Original jointed structure

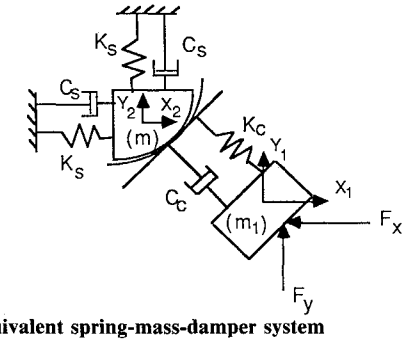

b) Equivalent spring-mass-damper system

Fig. 3 A jointed truss-cell unit structure and an equivalent system.

mental data.[15] In the later simulation study, the joint contact behaviors of the system with different system parameters (e.g., friction, joint clearance, joint stiffness/damping, link stiffness/damping) that are subjected to various excitations (e.g., excitation amplitude/frequency) are investigated. These analyses are summarized in three subjects: 1) joint contact pattern analysis, 2) joint contact force analysis, and 3) eigenvalue analysis.

Joint Contact Pattern Analysis

Figure 4 shows a typical joint contact pattern of the previous truss-cell model, which is obtained in a large clearance ($\delta = 1.0$ mm) and under a harmonic excitation ($\omega = 800$ rad/s). Detailed system parameters are also provided in Fig. 4. When the relative displacement $[(X_2 - X_1)^2 + (Y_2 - Y_1)^2]^{1/2}$ is greater than the clearance δ, the dynamic contact occurs. (In the contact pattern analysis, the other cases with different system parameters will be compared with Fig. 4.) The contact forces can be estimated from the mass penetration (which is physically impossible but numerically possible), and they will be presented next. In order to show the joint contacts clearly, the high-frequency excitation components were digitally filtered out in all the time histories presented thereafter.

A number of frequency components are observed in Fig. 4. The highest frequency, as indicated in circle 1, is associated with the joint contact oscillation (oscillation frequency at contact/unit time) determined by contact parameters $(K_c/m)^{1/2}$. The frequency component, in circle 2, before contact is related to the natural frequency of link oscillation $(K_s/m)^{1/2}$. The contact frequency (the number of contacts/unit time interval), the second lowest in circle 3, is determined by a number of factors, such as link stiffness/damping, contact stiffness/damping, joint clearance, and excitation amplitude/frequency. The lowest one (contact asymptote), the dashed line, is primarily determined by the joint friction and it disappears in the small clearance case. It is observed that, if other system parameters are fixed, reducing the friction coefficient (e.g., μ is decreased from 0.1 to 0.06) would result in even longer contact asymptote (lower asymptote frequency). The normal contact dominates at low friction and the friction contact dominates at high-friction value. This phenomena is also observed in the contact force analyses.

As discussed earlier, a number of system parameters affecting the contact pattern need to be investigated. Increasing the excitation amplitude results in more frequent contacts (higher contact frequency) and higher contact penetration (higher contact force). If the system is excited at one of the system natural frequencies, $(K_s/m)^{1/2}$ or $(K_c/m)^{1/2}$, the resonance effect can also appear, which results in higher contact force.

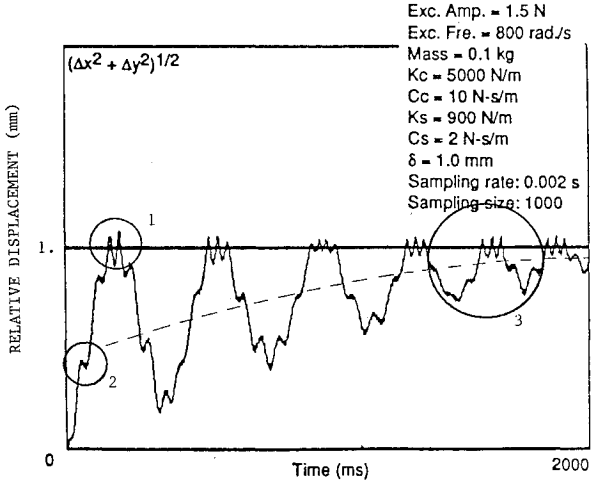

Fig. 4 Joint contact patterns.

Changes of equivalent link and contact parameters also affect the contact pattern (Figs. 5a and 5b). It shows that increasing the equivalent link stiffness results in higher contact frequency, and increasing contact stiffness results in higher amplitude oscillation after breaking the contact (Fig. 5a). Increasing equivalent system damping (both link and contact) weakens the dynamic contact and decreases contact frequency (Fig. 5b). It is observed that the contact asymptote did not change in all of these four cases. As discussed earlier, this contact asymptote is primarily affected by the joint friction; it disappears at very small joint clearance (because of the bouncing effect—contact at every cycle). Note that the previous time histories were compared with Fig. 4—the standard case.

Joint Contact Force Analysis

A contact force analysis using stochastic simulation is carried out to quantitatively evaluate the effect of changing system parameters. (It is assumed that the contact damping is larger than that of the link.) Figure 6a shows the effects of equivalent contact/link stiffness, and Fig. 6b shows the effects of contact/link damping. (Note that each data point shown in these figures is calculated using 10 test runs.) In general, the contact force increases with the increase of link/contact stiffness and decreases with the increase of link/contact damping. Note that, in the contact force analysis, random excitations were used.

As discussed previously, joint clearance and friction are also of importance to the contact dynamics. Figures 7 illustrate the clearance effect (with two different friction coefficients, i.e., $\mu = 0.1$ (Fig. 7a) and $\mu = 0.06$ (Fig. 7b). It is observed that, in very small joint clearance range, the contact force decreases as the clearance enlarges; in large clearance range, the contact force increases with the increase of joint clearance. In general,

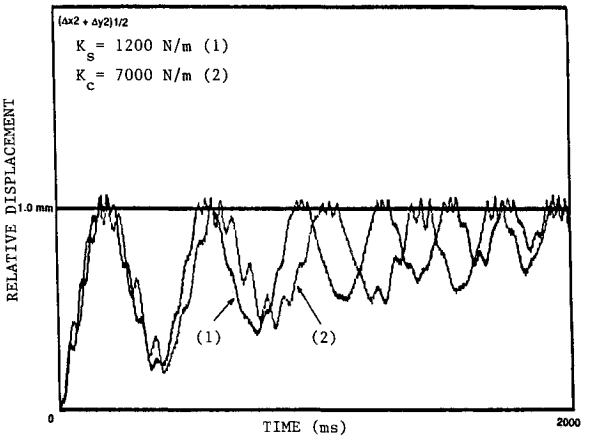

a) Change of equivalent joint/link stiffness

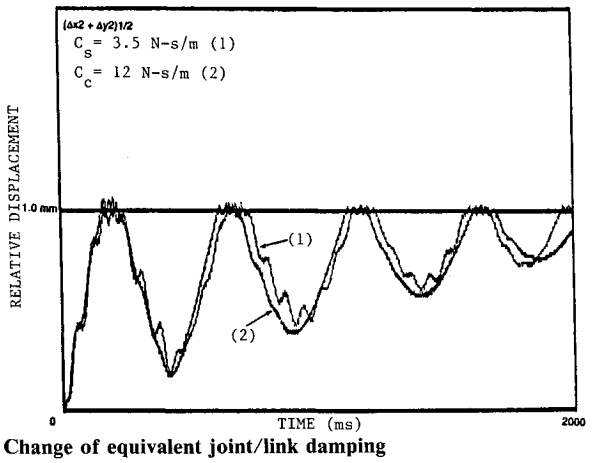

b) Change of equivalent joint/link damping

Fig. 5 Effect of equivalent joint/link stiffness/damping.

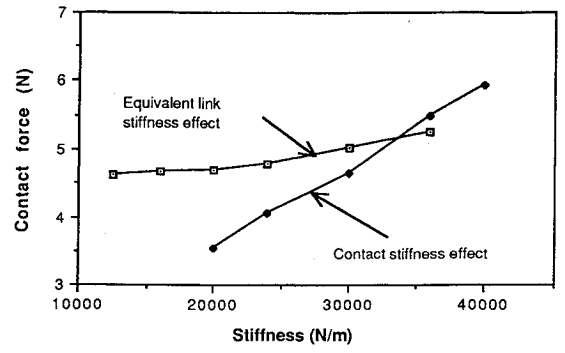

a) Effect of equivalent contact/link stiffness

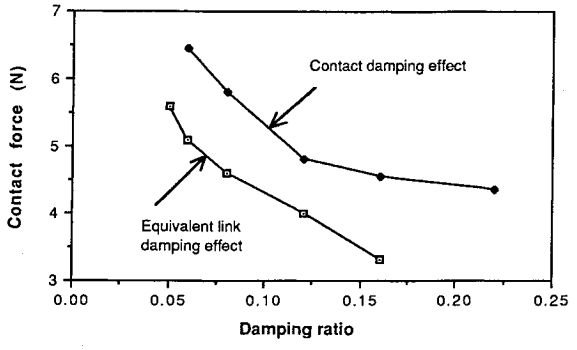

b) Effect of equivalent contact/link dampness

Fig. 6 Contact forces vs. equivalent contact/link stiffness/damping.

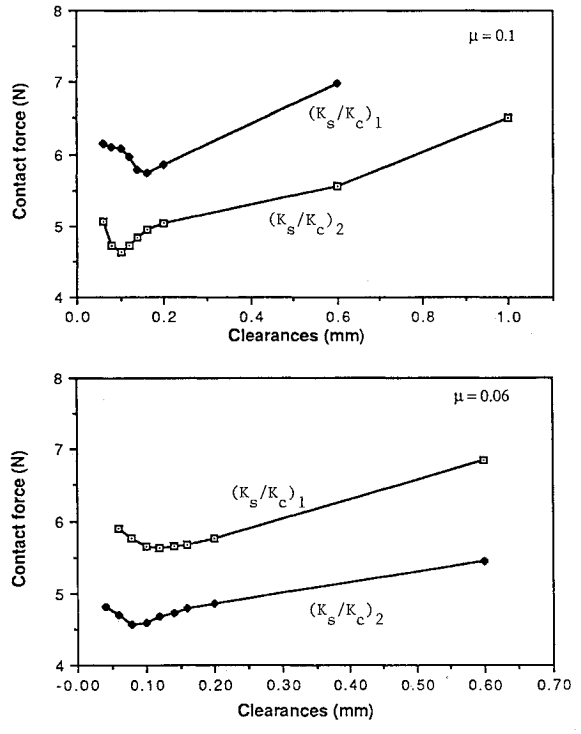

Fig. 7 Joint clearance and friction effects.

the contact force increases when the joint clearance enlarges. The similar phenomena were also observed in a study on elevator systems.[16] However, when considering very small joint clearance, some interesting phenomena are observed. The transition, the minimum contact force, shifts to the left when the friction decreases and shifts to the right when the

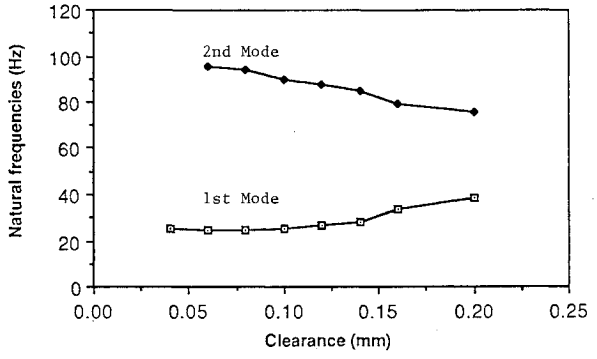

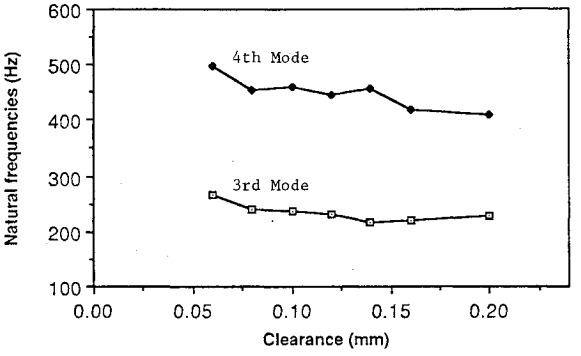

Fig. 8 Clearance effect on system frequencies.

contact/link stiffness increases. This is because the friction contact is more significant at small joint clearance and the normal contact is more significant at large clearance. At the transition, the effect of friction contact is balanced with that of the normal contact.

Eigenvalue Analysis

Natural frequencies of the system with elastic joint are also evaluated using a stochastic process—ARMA process. Figures 8 show that the frequencies change with respect to the joint clearance, which is calculated from the time-history data fitted into an ARMA model. The first modal frequency is related to the linear support parameters $(K_s/m)^{1/2}$. When the clearance is small, the two parts of the joint are not completely separated so that the first frequency is lower due to a combined mass effect, i.e., $[K_s/(m+m_1)]^{1/2}$. As the clearance enlarges, the two parts of the joint start separating so that the frequency approaches $(K_s/\mathrm{m})^{1/2}$. The second frequency is related to the contact parameters $(K_c/m)^{1/2}$, and the third and fourth are also associated with the contacts. They all decrease as the joint clearance enlarges (which means less contacts within a given time period).

Summary and Conclusions

In this paper, a mathematical model for a three-dimensional spherical joint was developed based on a contact force analysis, which includes the effects of normal contact and friction contact. The derived nonlinear joint equation has time-variant coefficient matrices depending on contact location, relative displacements, and step functions. This model was treated as a time-variant linear system so that a recursive algorithm was implemented to calculate the system responses. The simulation model was also randomized by including the friction variation (due to joint wear and aging) and by using random excitations in the simulation study. A stochastic simulation technique—an auto-regressive moving average (ARMA) process—was used to evaluate system performance when system parameters,

e.g., excitation frequency/amplitude, clearance size, link/joint stiffness, and damping, were specified. Based on the simulation study on a jointed truss-cell model, the following can be concluded.

1) The contact pattern of the system with an elastic joint is rather complicated; it is affected by a number of parameters, including excitation frequency/amplitude, clearance size, link stiffness/damping, contact stiffness/damping, lubrication, etc. In general, the contact oscillation is determined by the joint mass and the contact stiffness/damping. The oscillation before or after the contact is determined by the mass and the link stiffness/damping. Higher contact stiffness results in higher amplitude oscillation after breaking the contact. Higher damping (either link or contact) generally smooths out the joint contact. The contact asymptote is affected mainly by the joint friction. Higher joint friction contributes shorter asymptote.

2) It was also observed that the contact force, in general, increases as the joint clearance enlarges. However, at very small joint clearance, the friction contact dominates the joint vibration. A transition where the friction contact effect is balanced with that of the normal contact shows the minimum contact force. This transition point shifts when changing joint clearance and/or contact/link stiffness. Reducing the joint friction μ generally results in lower contribution of friction contact and higher contribution of normal contact in the overall joint contact dynamics. For a softer joint or more flexible link or higher joint/link damping, the contact force is generally smaller and the contact pattern is usually smoother.

3) The clearance variation also affects the natural frequencies of the system. The joint mass was not completely separated from the equivalent link mass at very small joint clearance. It was observed that the first natural frequency varies from $[K_s/(m+m_l)]^{1/2}$ to $[K_s/m]^{1/2}$ in the stochastic simulation study. The higher frequencies (second, third, and fourth modes) were all associated with the joint contact frequency, and they decrease as the clearance enlarges.

It should be noted that these results were obtained based on a quasistatic state approximation, in which large relative rotations are not considered. (This assumption should be reasonable for jointed space structures.) It was also assumed that the joint clearance is large enough to allow relative motion, i.e., joint sticktion phenomenon is not considered. As shown in the derived theoretical model, the system dynamics would be more complicated when the large rotations are included, which certainly needs to be further investigated. In practical applications, the joint parameters for a specific design also need to be identified before predicting reasonable system dynamics of the jointed structures. However, in general, these results and conclusions provide a microscopic physics that should be important to the joint clearance design and dynamic analysis of joint dominated flexible structures.

Acknowledgment

This research was supported, in part, by Grant 5-AM2 from the Center for Robotics and Manufacturing Systems (CRMS) at the University of Kentucky, Lexington, Kentucky. A research fellowship provided by the CRMS is also gratefully acknowledged. Comments from J. P. Sadler were appreciated.

References

[1]Rhodes, M. D., "Design Considerations for Joints in Deployable Space Truss Structures," First NASA/DOD CSI Tech. Conf., Norfolk, VA, Nov. 1986, pp. 383-398.

[2]Tzou, H. S., Hunter, R. M., and Gadre, M., "Dynamic Effect of Design Tolerance in High-Speed Machinery and Application of Viscoelastic Damping", *Procedings of the 1987 Symposium on Advanced Manufacturing*, Lexington, KY, Sept. 1987. pp. 111-116.

[3]Foelsche, G. A., Griffin, J. H., Bielak, J., "Transient Response of Joint-Dominated Space Structures: A New Linearization Technique," *AIAA Journal*, Vol. 26, No. 10, 1988, pp. 1278-1285.

[4]Crawley, E. F. and O'Donnell, K. J. "Force-State Mapping Identification of Nonlinear Joints," *AIAA Journal*, Vol. 25, No. 7, July 1987, pp. 1003-1022.

[5]Tzou, H. S., "Multibody Nonlinear Dynamics and Controls of Jointed Dominated Flexible Structures," Symposium on Robotics, ASME DSC, Vol. 11, Dec. 1988, pp. 6167.

[6]Rong, Y., Tzou, H. S. and Churng, C. S., "Theoretical Analysis and Simulation Study on Dynamic Behavior of Elastic Joints" *Proceedings of the International Conference of Machine Dynamics and Engineering Applications*, Xi'an, China, Aug. 27-31, 1988, pp. D32-37.

[7]Snyder, B. D., Burns, J. G., and Venkayya, V.B., "Composite Bolted Joints Analysis Programs," AIAA Paper 88-2423, April, 1988, pp. 1648-1655.

[8]Blackwood, G. H. and Von Flotow, A. H., "Experimental Component Mode Synthesis of Structures with Sloppy Joints," *Proceedings of the AIAA/ASME/ASCE 29th Structures Structural Dynamics and Materials Conference*, April 1988, pp. 1565-1575.

[9]Bowden, M. and Dugundji, J., "Effects of Joint Damping and Joint Nonlinearity on the Dynamics of Space Structures," AIAA Paper 88-2423, April 1988, pp. 1764-1773.

[10]Desai, U. B., *Modeling and Application of Stochastic Processes*, Kluwer, Boston, MA, 1986.

[11]Bell, R., and Anlagen, O., "The Friction Characteristics and the Sliding Stability of Machine Tool Slideways which Employ PTFE-Metal Composite Material," *Proceedings of the 19th International Machine Tool Design and Research Conference*, 1978.

[12]Banks, J., and Carson, J. S., *Discrete-Event System Simulation*, Prentice-Hall, Englewood Cliffs, NJ, 1984.

[13]Pandit, S. M. and Wu, S. M., *Time Series and System Analysis with Applications*, Wiley, New York, 1978.

[14]Box, G. E. P. and Jenkins, G. M., *Time Series Analysis, Forecasting and Control*, Holden-Day, San Francisco, CA, 1976.

[15]Tzou, H. S., "A Nonlinear Dynamic Analysis Finite Element Program with an Application to Elevator Counterweight System," Ph.D. Dissertation, Purdue Univ., West Lafayette, IN, 1983.

[16]Tzou, H. S. and Schiff, A.J., "Dynamics and Control of Elevators with Large Gaps and Rubber Damping," *ASCE Journal of Structural Engineering*, Vol. 115, No. 11, pp. 2753-2771, 1989.